buffered paraformaldehyde, removed from the coverslip, permeabilized for 6–12 h, incubated for 15 min in Alexa Fluor 488 streptavidin (Molecular Probes), washed again and mounted. Eight-bit image stacks were acquired on a confocal microscope (SP2; Leica) using the 40 × HCXP APO (numerical aperture 1.25) oil-immersion objective. Voxel size in the *xyz* dimension was $0.4 \times 0.4 \times 0.5\ \mu m^3$ ($0.05 \times 0.05 \times 0.5\ \mu m^3$ for high resolution). Measures of axonal arborization and diameter of the large mossy terminals were performed on montages of maximal intensity projections (Supplementary Fig. 1a) using ImageJ software (National Institute of Mental Health, Bethesda, Maryland). No further filtering or image processing was used.

Drugs and chemicals

MCPG and NBQX were purchased from Tocris Cookson, and ATP, CrP, EGTA, GTP, (−)-bicuculline methochloride and 3,3′-diaminobenzidine from Sigma/Fluka. (E)-4-(3-phosphonoprop-2-enyl)piperazine-2-carboxylic acid (CPPene) and CGP62349 were kindly provided by Novartis AG.

Data acquisition and analysis

Signals were filtered at 2 or 5 kHz, digitally recorded on a computer by using CLAMPEX 7 software (Axon Instruments) and stored on tape for later analysis. The amplitude, latency and kinetics were determined as described elsewhere[30]. To quantify the synaptic responses evoked by each action potential during a train, the peak amplitude and the area of the response were measured from the baseline directly preceding each EPSP. The standard deviation of the latencies was used to calculate the jitter. For calculation of the paired-pulse ratios, averages (including failures) were obtained. Numerical data in the text are expressed as means ± s.e.m.

Received 9 January; accepted 12 July 2004; doi:10.1038/nature02854.

1. Bischofberger, J. & Jonas, P. Two B or not two B: differential transmission at glutamatergic mossy fiber–interneuron synapses in the hippocampus. *Trends Neurosci.* **25,** 600–603 (2002).
2. Acsády, L., Kamondi, A., Sík, A., Freund, T. & Buzsáki, G. GABAergic cells are the major postsynaptic targets of mossy fibers in the rat hippocampus. *J. Neurosci.* **18,** 3386–3403 (1998).
3. Walker, M. C., Ruiz, A. & Kullmann, D. M. Monosynaptic GABAergic signaling from dentate to CA3 with a pharmacological and physiological profile typical of mossy fiber synapses. *Neuron* **29,** 703–715 (2001).
4. Zimmer, J. & Gähwiler, B. H. Cellular and connective organization of slice cultures of the rat hippocampus and fascia dentata. *J. Comp. Neurol.* **228,** 432–446 (1984).
5. Frotscher, M. & Gähwiler, B. H. Synaptic organization of intracellularly stained CA3 pyramidal neurons in slice cultures of rat hippocampus. *Neuroscience* **24,** 541–551 (1988).
6. Frotscher, M. Mossy fiber synapses on glutamate decarboxylase-immunoreactive neurons: evidence for feed-forward inhibition in the CA3 region of the hippocampus. *Exp. Brain Res.* **75,** 441–445 (1989).
7. Schwartzkroin, P. A., Scharfman, H. E. & Sloviter, R. S. Similarities in circuitry between Ammon's horn and dentate gyrus: local interactions and parallel processing. *Prog. Brain Res.* **83,** 269–286 (1990).
8. Spruston, N., Lübke, J. & Frotscher, M. Interneurons in the stratum lucidum of the rat hippocampus: an anatomical and electrophysiological characterization. *J. Comp. Neurol.* **385,** 427–440 (1997).
9. Siegel, S. J. *et al.* Regional, cellular, and ultrastructural distribution of *N*-methyl-D-aspartate receptor subunit 1 in monkey hippocampus. *Proc. Natl Acad. Sci. USA* **91,** 564–568 (1994).
10. Jonas, P., Major, G. & Sakmann, B. Quantal components of unitary EPSCs at the mossy fibre synapse on CA3 pyramidal cells of rat hippocampus. *J. Physiol. (Lond.)* **472,** 615–663 (1993).
11. Debanne, D., Guérineau, N. C., Gähwiler, B. H. & Thompson, S. M. Action-potential propagation gated by an axonal I_A-like K^+ conductance in hippocampus. *Nature* **389,** 286–289 (1997).
12. Miles, R. Synaptic excitation of inhibitory cells by single CA3 hippocampal pyramidal cells of the guinea-pig *in vitro*. *J. Physiol. (Lond.)* **428,** 61–77 (1990).
13. Debanne, D., Guérineau, N. C., Gähwiler, B. H. & Thompson, S. M. Physiology and pharmacology of unitary synaptic connections between pairs of cells in areas CA3 and CA1 of rat hippocampal slice cultures. *J. Neurophysiol.* **73,** 1282–1294 (1995).
14. Jung, M. W. & McNaughton, B. L. Spatial selectivity of unit activity in the hippocampal granular layer. *Hippocampus* **3,** 165–182 (1993).
15. Thompson, S. M. & Gähwiler, B. H. Activity-dependent disinhibition. I. Repetitive stimulation reduces IPSP driving force and conductance in the hippocampus *in vitro*. *J. Neurophysiol.* **61,** 501–511 (1989).
16. Brown, T. H. & Johnston, D. Voltage-clamp analysis of mossy fiber synaptic input to hippocampal neurons. *J. Neurophysiol.* **50,** 487–507 (1983).
17. Chicurel, M. E. & Harris, K. M. Three-dimensional analysis of the structure and composition of CA3 branched dendritic spines and their synaptic relationships with mossy fiber boutons in the rat hippocampus. *J. Comp. Neurol.* **325,** 169–182 (1992).
18. Geiger, J. R. & Jonas, P. Dynamic control of presynaptic Ca^{2+} inflow by fast-inactivating K^+ channels in hippocampal mossy fiber boutons. *Neuron* **28,** 927–939 (2000).
19. Llano, I. *et al.* Presynaptic calcium stores underlie large-amplitude miniature IPSCs and spontaneous calcium transients. *Nature Neurosci.* **3,** 1256–1265 (2000).
20. Liang, Y., Yuan, L. L., Johnston, D. & Gray, R. Calcium signaling at single mossy fiber presynaptic terminals in the rat hippocampus. *J. Neurophysiol.* **87,** 1132–1137 (2002).
21. Hallermann, S., Pawlu, C., Jonas, P. & Heckmann, M. A large pool of releasable vesicles in a cortical glutamatergic synapse. *Proc. Natl Acad. Sci. USA* **100,** 8975–8980 (2003).
22. Henze, D. A., Wittner, L. & Buzsáki, G. Single granule cells reliably discharge targets in the hippocampal CA3 network *in vivo*. *Nature Neurosci.* **5,** 790–795 (2002).
23. Miles, R. & Wong, R. K. Excitatory synaptic interactions between CA3 neurones in the guinea-pig hippocampus. *J. Physiol. (Lond.)* **373,** 397–418 (1986).
24. Nakazawa, K. *et al.* Requirement for hippocampal CA3 NMDA receptors in associative memory recall. *Science* **297,** 211–218 (2002).
25. Yeckel, M. F., Kapur, A. & Johnston, D. Multiple forms of LTP in hippocampal CA3 neurons use a common postsynaptic mechanism. *Nature Neurosci.* **2,** 625–633 (1999).
26. Kobayashi, K. & Poo, M. M. Spike train timing-dependent associative modification of hippocampal CA3 recurrent synapses by mossy fibers. *Neuron* **41,** 445–454 (2004).
27. Galarreta, M. & Hestrin, S. Frequency-dependent synaptic depression and the balance of excitation and inhibition in the neocortex. *Nature Neurosci.* **1,** 587–594 (1998).
28. Varela, J. A., Song, S., Turrigiano, G. G. & Nelson, S. B. Differential depression at excitatory and inhibitory synapses in visual cortex. *J. Neurosci.* **19,** 4293–4304 (1999).
29. Gähwiler, B. H., Thompson, S. M., McKinney, R. A., Debanne, D. & Robertson, R. T. in *Culturing Nerve Cells* 2nd edition (eds Banker, G. & Goslin, K.) 461–498 (MIT Press, Cambridge, Massachusetts, 1998).
30. Feldmeyer, D., Egger, V., Lübke, J. & Sakmann, B. Reliable synaptic connections between pairs of excitatory layer 4 neurones within a single 'barrel' of developing rat somatosensory cortex. *J. Physiol. (Lond.)* **521,** 169–190 (1999).

Supplementary Information accompanies the paper on **www.nature.com/nature**.

Acknowledgements We thank H. Blum, S. Giger, H. Kasper, L. Rietschin, and R. Schöb for technical assistance, and P. Streit for help in image processing. This work was funded by the Swiss National Science Foundation, the NCCR on Neural Plasticity and Repair, and the Hartmann Müller Foundation.

Competing interests statement The authors declare that they have no competing financial interests.

Correspondence and requests for materials should be addressed to M.M. (mori@hifo.unizh.ch).

Regulation of B-cell survival by BAFF-dependent PKCδ-mediated nuclear signalling

Ingrid Mecklenbräuker[1], Susan L. Kalled[2], Michael Leitges[3], Fabienne Mackay[4] & Alexander Tarakhovsky[1]

[1]*Laboratory of Lymphocyte Signaling, The Rockefeller University, New York, New York 10021, USA*
[2]*Biogen Idec, Inc., Cambridge, Massachusetts 02142, USA*
[3]*Max Planck Institute for Experimental Endocrinology, D 30625 Hannover, Germany*
[4]*Garvan Institute of Medical Research, St Vincent Hospital, Darlinghurst, NSW 2010, Sydney, Australia*

Approximately 65% of B cells generated in human bone marrow are potentially harmful autoreactive B cells[1]. Most of these cells are clonally deleted in the bone marrow, while those autoreactive B cells that escape to the periphery are anergized or perish before becoming mature B cells[2–5]. Escape of self-reactive B cells from tolerance permits production of pathogenic auto-antibodies[6]; recent studies suggest that extended B lymphocyte survival is a cause of autoimmune disease in mice and humans[7]. Here we report a mechanism for the regulation of peripheral B-cell survival by serine/threonine protein kinase Cδ (PKCδ): spontaneous death of resting B cells is regulated by nuclear localization of PKCδ that contributes to phosphorylation of histone H2B at serine 14 (S14-H2B). We show that treatment of B cells with the potent B-cell survival factor BAFF ('B-cell-activating factor belonging to the TNF family') prevents nuclear accumulation of PKCδ. Our data suggest the existence of a previously unknown BAFF-induced and PKCδ-mediated nuclear signalling pathway which regulates B-cell survival.

The increased lifespan of B cells in transgenic mice that overexpress the B-cell survival factor BAFF is associated with development of lupus-like autoimmunity[8–10]. We recently described a lupus-like autoimmune disease with defective B-cell tolerance in mice deficient for PKCδ[11]. In searching for the mechanism of the disease, we found that PKCδ-deficiency renders B cells BAFF-independent. Injection of a soluble BAFF receptor-Fc decoy, BAFF-R:Fc[12], in $PKC\delta^{+/+}$ mice reduces the cellularity of the lymphoid organs (Fig. 1a, upper panel) by emptying peripheral

B-cell compartments and blocking most B-cell maturation at the transitional 1 (T1) (IgM^+CD21^-) stage (Fig. 1b, upper panel). Unlike $PKC\delta^{+/+}$ mice, injection of the soluble BAFF receptor into PKCδ-deficient mice has no effect on either the size of the B-cell compartment or B-cell survival and maturation (Fig. 1a and b, upper panels).

The independence of $PKC\delta^{-/-}$ B cells on BAFF was confirmed by analysis of B-cell subpopulations in mice in which PKCδ-deficiency is combined with a loss-of-function mutation in the BAFF receptor (BAFF-R). To produce these mice, the $PKC\delta^{-/-}$ mice were bred to A/WySnJ mutant mice that express a signalling-incompetent form of the BAFF-R[13,14]. In the presence of PKCδ, lack of BAFF signalling leads to reduction in the size of the lymphoid organs (Fig. 1a, lower panel), a decline in peripheral B-cell numbers (Fig. 1c) and a partial block in the maturation of immature (IgM^+CD21^-) to mature (IgM^+CD21^+) B cells (Fig. 1b, lower panel). In contrast to $PKC\delta^{+/+}$ A/WySnJ mice, $PKC\delta^{-/-}$ A/WySnJ mice have even more splenic and lymph node B cells and display a normal pattern of peripheral B-cell maturation (Fig. 1b and c, and data not shown). The recovery of the peripheral B-cell compartment in the absence of PKCδ cannot be attributed to higher expression of BAFF-R as PKCδ-deficient B cells have wild-type levels of BAFF-R messenger RNA (Supplementary Fig. 1a) and BAFF levels in the serum of the $PKC\delta^{-/-}$ mice are within $PKC\delta^{+/+}$ limits (Supplementary Fig. 1b).

The greater than wild-type size of the $PKC\delta^{-/-}$ B-cell compartment in the absence of BAFF signalling could be due to the increased lifespan of PKCδ-deficient B cells *in vitro* and *in vivo* (Fig. 2a and c). Most $PKC\delta^{+/+}$ B cells cultured in serum-containing medium die within 3–4 days (Fig. 2a). PKCδ-deficiency renders B cells less susceptible to spontaneous death; about 20% remain alive even on day 14 of culture (Fig. 2a). Increased survival of the PKCδ-deficient B cells is not due to increased production of pro-survival cytokines such as interleukin-6 (IL-6). In the absence of stimulation, both $PKC\delta^{+/+}$ and PKCδ-deficient B cells express equal levels of IL-6 mRNA, and secrete similar amounts of IL-6 (Supplementary Fig. 2a). Furthermore, *in vitro* depletion of IL-6 with a neutralizing anti-IL-6 antibody does not affect the survival of PKCδ-deficient B cells (Supplementary Fig. 2b). The PKCδ-deficient B cells that survive *in vitro* for 14 days are functional and can be activated to proliferate by anti-IgM with IL-4, bacterial lipopolysaccharide (LPS), or unmethylated oligonucleotide (CpG) with kinetics similar to activation of freshly isolated $PKC\delta^{+/+}$ or PKCδ-deficient B cells (Fig. 2b).

It is possible that PKCδ controls B-cell survival in a BAFF-independent fashion and survival of PKCδ-deficient B cells reflects the general pro-apoptotic activity of PKCδ. To test this model, we generated mice in which PKCδ-deficiency is combined with Btk-

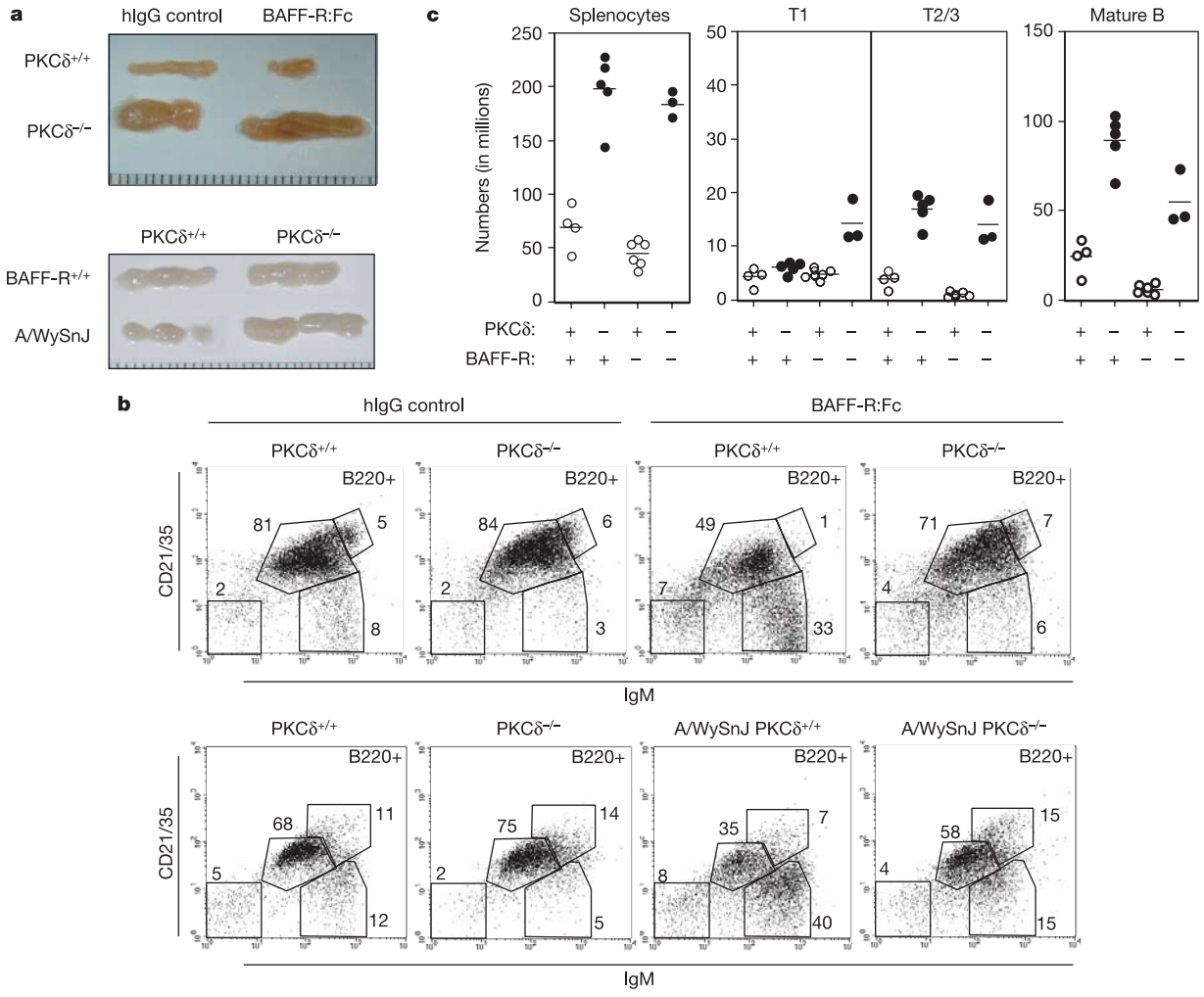

Figure 1 PKCδ-deficient B cells are independent of BAFF. **a**, Lymph nodes of mice injected with soluble BAFF-R:Fc (upper panel) or of 8-week-old A/WySnJ $PKC\delta^{-/-}$ or littermate control mice (lower panel) are shown. **b**, **c**, PKCδ-deficiency releases the block in B-cell maturation in the absence of BAFF signalling. **b**, Maturity of splenic B cells was assessed by analysis of the surface expressed CD21/35 and IgM. Data are representative of three independent experiments. **c,** Absolute numbers of splenic $CD19^+$ immature (IgM^+CD21^-) and mature (IgM^+CD21^+) B cells of A/WySnJ $PKC\delta^{+/+}$ (open symbols) or A/WySnJ $PKC\delta^{-/-}$ (filled symbols) mice are shown. Each dot represents an individual mouse.

deficiency[15]. The latter mutation causes a major decline in the survival of naïve B cells *in vitro*; this can be reversed by over-expression of the Bcl-2 protein[16]. Our data show that PKCδ-deficiency fails to rescue poor survival (Fig. 2d) and B-cell cellularity in the lymphoid organs of the PKCδ$^{-/-}$ Btk$^{-/-}$ mice (Fig. 2e and data not shown). The existence of a PKCδ-dependent pro-apoptotic pathway that operates via potentially novel signalling mechanisms is also supported by Affymetrix gene chip and RT–PCR analyses, which show no significant differences in the PKCδ-deficient and PKCδ$^{+/+}$ B cells in expression of mRNAs encoding known anti- or pro-apoptotic proteins (Supplementary Fig. 3a). Furthermore, deficiency in PKCδ does not affect BAFF-mediated processing of the NF-κB2 that was previously implicated in positive regulation of B-cell survival[17,18] (Supplementary Fig. 3b). Collectively, these results exclude a general anti-apoptotic effect of PKCδ-deficiency and suggest a specific BAFF-dependent pathway that regulates B-cell survival by negative regulation of PKCδ.

Previous studies on the role of PKCδ in cell death revealed a pro-apoptotic function of this enzyme in cells of various types[19]. It was shown that initiation of apoptosis caused by various agents correlates with nuclear translocation of the full-length PKCδ (PKCδ-FL) or its catalytic fragment (PKCδ-CF), generated by caspase-3-mediated cleavage at the site that separates the regulatory and the catalytic subunits of the enzyme[20,21]. The pro-apoptotic activity of PKCδ requires nuclear localization[22] and correlates directly with its enzymatic activity; this is demonstrated by differences in the efficiency of cell death induction by expression of exogenous PKCδ-FL and PKCδ-CF, which possess higher enzymatic activity than non-cleaved PKCδ-FL[23]. These findings, as well as the failure of catalytically inactive PKCδ to cause cell death[22], suggest that the pro-apoptotic function of PKCδ is mediated through phosphorylation of nuclear targets.

In *ex vivo* isolated splenic B cells, the majority of the PKCδ protein is located in the cytosol (Fig. 3a). However, 24 h incubation of B cells in serum-containing medium, which triggers some of the B cells to death (Fig. 2a), leads to an increase in nuclear PKCδ-FL (Fig. 3a). This process is independent of the activity of caspases that are implicated in cell death. Incubation of *ex vivo* isolated B cells with the pan-caspase inhibitor Z-VAD-FMK or with inhibitors specific for caspase-3, -6 or–9 does not prevent nuclear accumulation of PKCδ-FL (Fig. 3b and data not shown). Whereas the role of caspases in cell death is obvious, our data suggest that nuclear

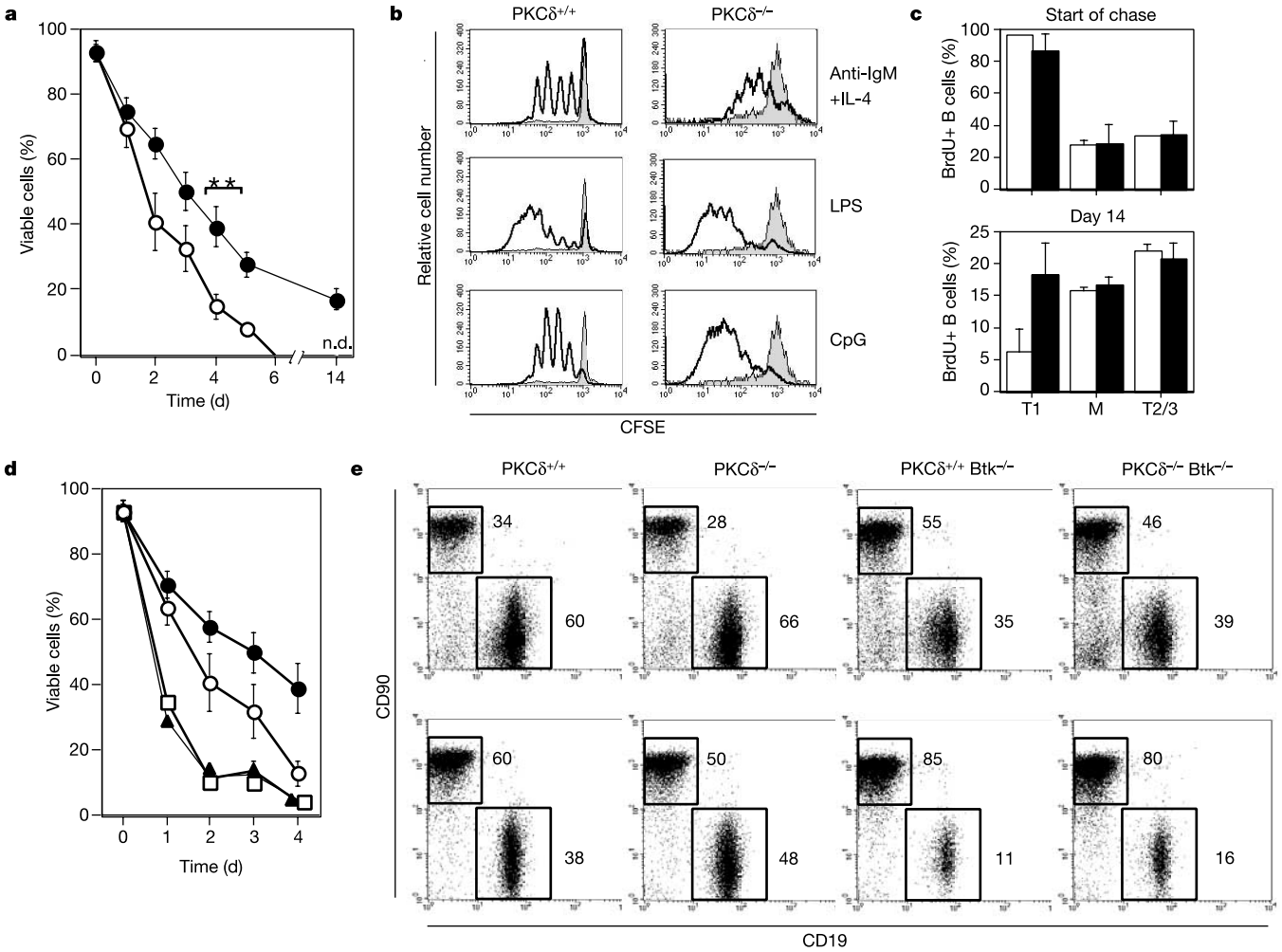

Figure 2 PKCδ promotes B-cell survival. **a**, B-cell survival *in vitro*. Frequencies of viable PKCδ$^{+/+}$(open circles) or PKCδ$^{-/-}$ (filled circles) B cells incubated in medium. Data are means ± s.d. from 5–10 independent experiments. n.d., not detectable. $^{**}P < 0.0001$ by *t* test. **b**, Proliferation of freshly isolated PKCδ$^{+/+}$ or PKCδ$^{-/-}$ B cells (day 14 after culture) in the absence (grey histogram) or presence of stimuli (thick line) was measured by CFDA-SE labelling. **c**, B-cell lifespan *in vivo* was measured by BrdU incorporation. Open bars, PKCδ$^{+/+}$; filled bars, PKCδ$^{-/-}$. Data are means ± d.f. from three mice. **d** and **e**, PKCδ-deficiency does not rescue the survival of Btk-deficient B cells. **d**, Frequencies of viable B cells after incubation in medium. Open circles, PKCδ$^{+/+}$Btk$^{+/+}$; filled circles, PKCδ$^{-/-}$Btk$^{+/+}$; open squares, Btk$^{-/-}$; filled triangles, PKCδ$^{-/-}$Btk$^{-/-}$. Data are means ± s.d. from two independent experiments. **e**, Frequencies of splenic (upper panel) and lymph node (lower panel) T (CD90^{+}) and B (CD19^{+}) cells.

translocation of PKCδ and hence related to it B-cell death, are caspase-independent. It is possible that BAFF regulates B-cell survival through negative regulation of nuclear PKCδ. Indeed, we found that treatment of B cells with recombinant BAFF prevents nuclear accumulation of PKCδ (Fig. 3a).

The connection between PKCδ translocation to the nucleus and cell death raises the question of nuclear targets for PKCδ. Within the nucleus, the most abundant PKC substrates are histones. It has been shown that phosphorylation of histone H2B at serine 14 (S14-H2B) is associated with cell death[24,25]. We therefore hypothesized that the ability of PKCδ to induce apoptosis might reflect its ability to phosphorylate S14 of the histone H2B.

Expression of the exogenous PKCδ catalytic fragment (PKCδ-CF) in NIH3T3 cells and in PKCδ$^{+/+}$ or PKCδ-deficient embryonic fibroblasts increases S14-H2B phosphorylation to levels higher than those observed in non-transfected cells (or in cells transfected with either the full-length PKCδ or a PKCδ variant that lacks the caspase-cleavage site) (Fig. 4a and b). The overall higher levels of S14-H2B phosphorylation in NIH3T3 cells that express various PKCδ variants is likely to reflect the higher expression levels of the PKCδ–GFP fusion proteins in NIH3T3 cells as compared to embryonic fibroblasts. In lymphoid cells S14-H2B appears to be a specific substrate for PKCδ, as neither phosphorylation of serine 10 (S10-H3) nor serine 28 (S28-H3) of histone H3 is affected by expression of highly pro-apoptotic PKCδ-CF (Fig. 4c). Involvement of PKCδ in S14-H2B phosphorylation is further supported by the analysis of *ex vivo* isolated peripheral resting B cells (Fig. 4d). The S14-H2B phosphorylation could be detected in freshly isolated PKCδ$^{+/+}$ B cells that do not contain nuclear PKCδ. Hence kinases other than PKCδ can also contribute to S14-H2B phosphorylation in B cells. One of them could be the *sterile twenty kinase* Mst1 that can phosphorylate S14-H2B in mammalian cells[25]. Nonetheless, the significantly reduced levels of S14-H2B phosphorylation in PKCδ-deficient B cells points to a major contribution of PKCδ to regulation of S14-H2B phosphorylation in resting B cells (Fig. 4d). Appearance of phosphorylated S14-H2B is unlikely to be the consequence of apoptosis as such. Thus apoptotic death of PKCδ$^{+/+}$ B cells induced by anti-Fas antibody is not associated with an increase in S14-H2B phosphorylation (Fig. 4e). This result, along with our data on unaltered PKCδ$^{-/-}$ B-cell sensitivity to Fas-mediated death[11], point to a specific role of PKCδ and S14-H2B phosphorylation in spontaneous B-cell death.

Whereas our data reveal an important role of PKCδ in regulation of S14-H2B phosphorylation, the role of S14-H2B phosphorylation in B-cell death remains unclear. The presence of multiple H2B genes

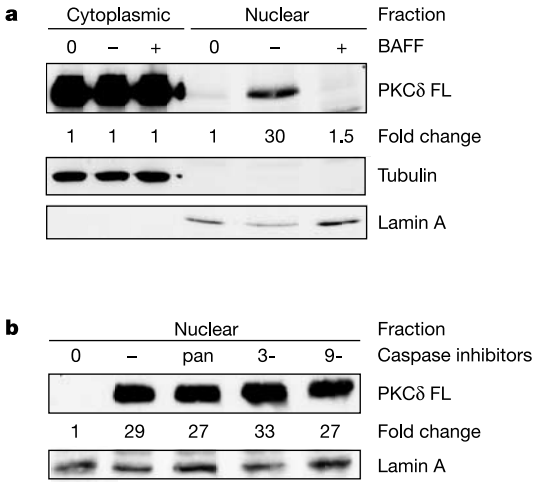

Figure 3 Nuclear expression of PKCδ in *ex vivo* isolated B cells is negatively regulated by BAFF. Purified B cells were incubated for 24 h in serum-containing medium in the absence or presence of BAFF (**a**), or with pan-, caspase-3 or -9-specific inhibitors (**b**), followed by preparation of cytosolic and nuclear extracts. Expression of PKCδ was measured by western blot analysis of extracts using anti-PKCδ antibody. Protein loading was controlled by tubulin and lamin A expression analysis. 0, freshly isolated cells. Data were quantified by NIH Image software.

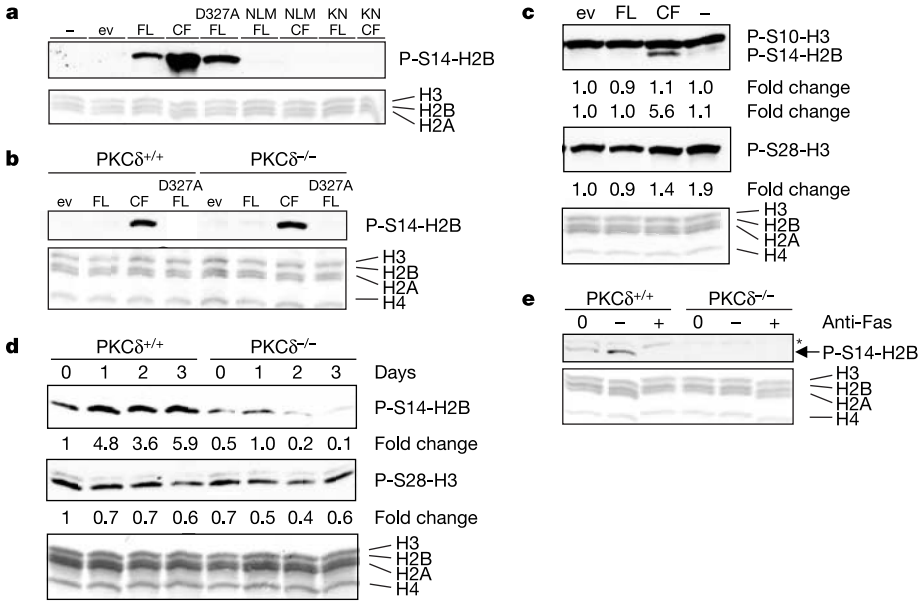

Figure 4 PKCδ contributes to cell-death-related phosphorylation of S14-H2B. **a**–**c**, The levels of histone phosphorylation were measured by western blot analysis using phospho- and residue-specific antibodies in NIH3T3 cells (**a**); mouse embryonic fibroblasts generated from PKCδ$^{+/+}$ and PKCδ$^{-/-}$ mice (**b**); murine A20 cells (**c**) overexpressing full-length (FL), catalytic fragment (CF), caspase-cleavage-deficient (D327A), nuclear localization sequence (NLM)-deficient or kinase-inactive (KN) PKCδ. Protein loading was controlled by Ponceau staining of core histones. –, not infected; ev, empty vector. **d**, Purified PKCδ$^{+/+}$ and PKCδ$^{-/-}$ B cells were incubated in serum-containing medium for different time periods. The levels of S14-H2B and S28-H3 phosphorylation were measured by western blot analysis. Data were quantified by NIH Image software. **e**, Not-activated (–) or anti-CD40-triggered (+) purified PKCδ$^{+/+}$ and PKCδ$^{-/-}$ splenic B cells were subjected to anti-Fas antibody treatment for 6 h. The level of S14-H2B phosphorylation was measured by western blot analysis. 0, freshly isolated cells.

in the mouse genome precludes analysis of the physiological role of S14-H2B phosphorylation by mutagenesis *in vivo*. Nonetheless, attenuation of hydrogen-peroxide-induced cell death by replacement of S14-H2B of *Saccharomyces cerevisiae* (S. H. Ahn and D. Allis, personal communication), and recent data that show accumulation of the S14-H2B at sites of DNA breaks[26], indicate the importance of P-S14-H2B in apoptosis. Should S14-H2B phosphorylation determine the rate of spontaneous B-cell death, then the lower levels of S14-H2B phosphorylation in the absence of PKCδ may explain slower (compared to PKCδ$^{+/+}$ B cells) kinetics of PKCδ-deficient B cell death *in vitro*.

In conclusion, our results show that BAFF promotes B-cell survival not only through the NF-κB-mediated increase in the expression of anti-apoptotic proteins, but also by actively preventing nuclear translocation of PKCδ. □

Methods

Mice

Mice with PKCδ-deficiency[11], initially on 129/Sv*Ola background, were backcrossed to C57BL/6 mice for at least 10 generations. PKCδ$^{+/-}$ mice were intercrossed to generate mutant and control mice. The predominant C57BL/6 genetic background of PKCδ$^{-/-}$ mice was verified by microsatellite genotyping performed at the Rockefeller University Genotyping Resource Center (Supplementary Table 1). BAFF-R mutant PKCδ$^{-/-}$ or Btk$^{-/-}$PKCδ-doubly-deficient mice and the corresponding littermate control mice were generated by crossing either PKCδ-deficient and A/WySnJ mice (The Jackson Laboratory) or PKCδ-deficient and Btk$^{-/-}$ mice (The Jackson Laboratory) and intercrossing the resulting F1 mice to generate F2. For neutralization of BAFF, 30-week-old littermate PKCδ-deficient or PKCδ$^{+/+}$ were injected i.p. with 100 μg of control-Ig (human IgG, Novartis) or with BAFF-R:Fc[12] three times a week for five weeks. For 5-bromo-2-deoxyuridine (BrdU) labelling, PKCδ$^{+/+}$ and PKCδ-deficient mice received 1 mg ml^{-1} of BrdU in their drinking water for 14 days. BrdU incorporation into B cells was determined by staining with FITC-labelled anti-BrdU antibody (BD Pharmingen). Frequency of BrdU^{+} B cells was measured by flow cytometry.

Cell lines, transient transfections, nuclear extract preparation

Mouse embryonic fibroblasts were generated from 13.5-day PKCδ$^{+/+}$ and PKCδ$^{-/-}$ embryos by standard procedure. Transfection of NIH3T3, Jurkat, BJAB, Ramos and A20 cells was done either according to the Lipofectamine Plus kit (Invitrogen) or by electroporation. Seventy-two hours after transfection with various constructs[22], cells were washed with PBS and lysed as described[27]. Briefly, cells were lysed for 15 min on ice in 320 mM sucrose, 10 mM Tris pH 8.0, 3 mM $CaCl_2$, 2 mM magnesium acetate, 0.1 mM EDTA, 0.5% NP-40, supplemented with protease (Sigma) and phosphatase (Calbiochem) inhibitor cocktails. After 5 min of centrifugation at 500*g*, supernatants were saved as the cytosolic fraction. The nuclei were washed in the same buffer without NP-40 and then lysed in 1% NP-40, 500 mM NaCl, 50 mM Tris pH 8.0, 10% glycerol, and sonificated. The supernatants after 15 min of centrifugation at 16×10^3g were used as nuclear fraction.

Immunoblotting analysis

Western blot analysis was performed by separating equal amounts of protein extracts by SDS–PAGE and blotting to nitrocellulose membrane by standard procedures. For immunoblotting of cytoplasmic and nuclear PKCδ, protein extracts of purified B cells were analysed by immunoblotting with an antibody against PKCδ (Santa Cruz). Protein loading was controlled with anti-lamin A antibody (Cell Signaling) and anti-tubulin antibody (Sigma). The expression of p100 and p52 of NF-κB2 was studied using protein extracts prepared as described[18] and antibodies against NF-κB2 (Upstate) or β-actin (Oncogene). For immunoblotting of nuclear histones, protein loading was controlled by reversible staining of the core histones H3, H2B, H2A and H4 on the membrane with Ponceau S solution (Sigma), followed by probing with phospho-specific antibodies against S14-H2B, S10-H3 and S28-H3 (Upstate). Data were quantified by NIH Image software.

B-cell purification, proliferation, staining and flow cytometry

Splenic B cells were purified as described previously[11] and stimulated *in vitro* with 2.4 μg ml^{-1} F(ab′)$_2$ fragment of goat anti-mouse IgM (Jackson ImmunoResearch) in combination with 25 U ml^{-1} recombinant mouse IL-4 (R&D), 5 μg ml^{-1} bacterial LPS (Sigma), or 10 nM CpG ODN 1638 (MWG Biotech). For neutralization of any IL-6 bioactivity, purified rat anti-mouse IL-6 (MP5-20F3) and rat IgG1 isotype-matched control (R3-34) antibodies (BD Pharmingen) were used. The caspase inhibitors Z-VAD-FMK, Z-VEID-FMK, Z-LEHD-FMK (BioVision) and DEVD-CHO (Biosource) were used at a concentration of 100 nM. For induced apoptosis, purified B cells were activated with 0.6 μg ml^{-1} anti-CD40 antibody for 12 h and then subjected to 50 ng ml^{-1} anti-Fas antibody treatment. Labelling of cells with 5-(and 6-)-carboxyfluorescein diacetate, succinimidyl ester (CFDA-SE; Molecular Probes) for analysis of proliferation was performed as described[11]. The decline in CFSE fluorescence as a measure of B-cell proliferation was determined by FACS analysis. Lymphocyte surface marker expression was analysed using monoclonal antibodies against CD19, CD21/35, CD23, CD90, B220 (BD Pharmingen) or F(ab′)$_2$ fragment of goat anti-mouse IgM (Jackson ImmunoResearch) as described previously[11].

Construction and generation of MigRI-PKCδ retroviruses

Construction of the GFP-tagged PKCδ-FL, its catalytic fragment (PKCδ-CF), caspase-cleavage mutant (D327A), or PKCδ with mutated nuclear localization sequence (NLM), or dominant-negative (K376R) PKCδ were described previously[22]. The PKCδ–GFP fusions were excised with Not*I* and Xho*I*, blunt-ended and ligated into the MigRI vector[28] after removing the IRES–GFP. The infectious retroviral particles were then produced by cotransfecting retrovirus vector DNA with the helper plasmid pCL-Eco into Bosc23 packaging cells. Retroviral supernatants were collected and filtered 48 h later. The PKCδ$^{+/+}$ and PKCδ$^{-/-}$ MEFs were then infected with the supernatant with 8 μg ml^{-1} polybrene (Sigma). Aliquots of cells were either subjected to FACS analysis for GFP expression or lysed 48 h post-infection.

Cell survival assay

Purified B cells were cultured either in medium alone or in the presence of 500 ng ml^{-1} of recombinant BAFF[29] for the indicated time and stained with Annexin V (Roche) and 7-aminoactinomycin D (7-AAD; Sigma-Aldrich)[30].

Received 12 July; accepted 16 August 2004; doi:10.1038/nature02955.
Published online 8 September 2004.

1. Wardemann, H. *et al.* Predominant autoantibody production by early human B cell precursors. *Science* **301,** 1374–1377 (2003).
2. Goodnow, C. C. *et al.* Altered immunoglobulin expression and functional silencing of self-reactive B lymphocytes in transgenic mice. *Nature* **334,** 676–682 (1988).
3. Nemazee, D. A. & Burki, K. Clonal deletion of B lymphocytes in a transgenic mouse bearing anti-MHC class I antibody genes. *Nature* **337,** 562–566 (1989).
4. Erikson, J. *et al.* Expression of anti-DNA immunoglobulin transgenes in non-autoimmune mice. *Nature* **349,** 331–334 (1991).
5. Hartley, S. B. *et al.* Elimination from peripheral lymphoid tissues of self-reactive B lymphocytes recognizing membrane-bound antigens. *Nature* **353,** 765–769 (1991).
6. Goodnow, C. C. Balancing immunity and tolerance: deleting and tuning lymphocyte repertoires. *Proc. Natl Acad. Sci. USA* **93,** 2264–2271 (1996).
7. Mackay, F. & Kalled, S. L. TNF ligands and receptors in autoimmunity: an update. *Curr. Opin. Immunol.* **14,** 783–790 (2002).
8. Mackay, F. *et al.* Mice transgenic for BAFF develop lymphocytic disorders along with autoimmune manifestations. *J. Exp. Med.* **190,** 1697–1710 (1999).
9. Gross, J. A. *et al.* TACI and BCMA are receptors for a TNF homologue implicated in B-cell autoimmune disease. *Nature* **404,** 995–999 (2000).
10. Khare, S. D. *et al.* Severe B cell hyperplasia and autoimmune disease in TALL-1 transgenic mice. *Proc. Natl Acad. Sci. USA* **97,** 3370–3375 (2000).
11. Mecklenbräuker, I., Saijo, K., Zheng, N. Y., Leitges, M. & Tarakhovsky, A. Protein kinase Cδ controls self-antigen-induced B-cell tolerance. *Nature* **416,** 860–865 (2002).
12. Pelletier, M. *et al.* Comparison of soluble decoy IgG fusion proteins of BAFF-R and BCMA as antagonists for BAFF. *J. Biol. Chem.* **278,** 33127–33133 (2003).
13. Thompson, J. S. *et al.* BAFF-R, a newly identified TNF receptor that specifically interacts with BAFF. *Science* **293,** 2108–2111 (2001).
14. Yan, M. *et al.* Identification of a novel receptor for B lymphocyte stimulator that is mutated in a mouse strain with severe B cell deficiency. *Curr. Biol.* **11,** 1547–1552 (2001).
15. Khan, W. N. *et al.* Defective B cell development and function in Btk-deficient mice. *Immunity* **3,** 283–299 (1995).
16. Woodland, R. T., Schmidt, M. R., Korsmeyer, S. J. & Gravel, K. A. Regulation of B cell survival in xid mice by the proto-oncogene bcl-2. *J. Immunol.* **156,** 2143–2154 (1996).
17. Claudio, E., Brown, K., Park, S., Wang, H. & Siebenlist, U. BAFF-induced NEMO-independent processing of NF-κB2 in maturing B cells. *Nature Immunol.* **3,** 958–965 (2002).
18. Kayagaki, N. *et al.* BAFF/BLyS receptor 3 binds the B cell survival factor BAFF ligand through a discrete surface loop and promotes processing of NF-κB2. *Immunity* **17,** 515–524 (2002).
19. Mischak, H. *et al.* Overexpression of protein kinase C-δ and -ε in NIH3T3 cells induces opposite effects on growth, morphology, anchorage dependence, and tumorigenicity. *J. Biol. Chem.* **268,** 6090–6096 (1993).
20. Emoto, Y. *et al.* Proteolytic activation of protein kinase C δ by an ICE-like protease in apoptotic cells. *EMBO J.* **14,** 6148–6156 (1995).
21. Ghayur, T. *et al.* Proteolytic activation of protein kinase C δ by an ICE/CED 3-like protease induces characteristics of apoptosis. *J. Exp. Med.* **184,** 2399–2404 (1996).
22. DeVries, T. A., Neville, M. C. & Reyland, M. E. Nuclear import of PKCδ is required for apoptosis: identification of a novel nuclear import sequence. *EMBO J.* **21,** 6050–6060 (2002).
23. Reyland, M. E., Anderson, S. M., Matassa, A. A., Barzen, K. A. & Quissell, D. O. Protein kinase C δ is essential for etoposide-induced apoptosis in salivary gland acinar cells. *J. Biol. Chem.* **274,** 19115–19123 (1999).
24. Ajiro, K. Histone H2B phosphorylation in mammalian apoptotic cells. An association with DNA fragmentation. *J. Biol. Chem.* **275,** 439–443 (2000).
25. Cheung, W. L. *et al.* Apoptotic phosphorylation of histone H2B is mediated by mammalian sterile twenty kinase. *Cell* **113,** 507–517 (2003).
26. Fernandez-Capetillo, O., Allis, C. D. & Nussenzweig, A. Phosphorylation of histone H2B at DNA double-strand breaks. *J. Exp. Med.* **199,** 1671–1677 (2004).
27. Su, I. H. *et al.* Ezh2 controls B cell development through histone H3 methylation and Igh rearrangement. *Nature Immunol.* **4,** 124–131 (2003).
28. Van Parijs, L. *et al.* Uncoupling IL-2 signals that regulate T cell proliferation, survival, and Fas-mediated activation-induced cell death. *Immunity* **11,** 281–288 (1999).
29. Karpusas, M. *et al.* Crystal structure of extracellular human BAFF, a TNF family member that stimulates B lymphocytes. *J. Mol. Biol.* **315,** 1145–1154 (2002).
30. Saijo, K. *et al.* Protein kinase Cβ controls nuclear factor κB activation in B cells through selective regulation of the IκB kinase α. *J. Exp. Med.* **195,** 1647–1652 (2002).

Supplementary Information accompanies the paper on **www.nature.com/nature**.

Acknowledgements We thank S. H. Ahn, D. Allis, M. Reyland, U. Siebenlist, the Rockefeller University Genotyping Resource Center and the MSKCC Genomics Core Laboratory for providing cells, vectors, reagents and technical assistance. We also thank E. Besmer for help with manuscript preparation, and A. Patke and members of the Tarakhovsky laboratory for discussions. This work was supported by The Irene Diamond Fund/Professorship Program (A.T.), the NIH (A.T.) and The S.L.E. Foundation (I.M.).

Competing interests statement The authors declare that they have no competing financial interests.

Correspondence and requests for materials should be addressed to A.T. (tarakho@mail.rockefeller.edu).

NF-κB functions as a tumour promoter in inflammation-associated cancer

Eli Pikarsky[1]*, Rinnat M. Porat[1]*, Ilan Stein[1,2]*, Rinat Abramovitch[3], Sharon Amit[2], Shafika Kasem[1], Elena Gutkovich-Pyest[2], Simcha Urieli-Shoval[4], Eithan Galun[3] & Yinon Ben-Neriah[2]

[1]*Department of Pathology, Hadassah-Hebrew University Medical Center, Jerusalem 91120, Israel*
[2]*The Lautenberg Center for Immunology, Hebrew University-Hadassah Medical School, Jerusalem 91120, Israel*
[3]*Goldyne Savad Institute of Gene Therapy, Jerusalem 91120, Israel*
[4]*Hematology Unit, Hadassah University Hospital, Mount Scopus, Jerusalem 91120, Israel*

* These authors contributed equally to this work

The causes of sporadic human cancer are seldom recognized, but it is estimated that carcinogen exposure and chronic inflammation are two important underlying conditions for tumour development, the latter accounting for approximately 20% of human cancer[1]. Whereas the causal relationship between carcinogen exposure and cancer has been intensely investigated[2], the molecular and cellular mechanisms linking chronic inflammation to tumorigenesis remain largely unresolved[1]. We proposed that activation of the nuclear factor κB (NF-κB), a hallmark of inflammatory responses[3] that is frequently detected in tumours[4,5], may constitute a missing link between inflammation and cancer. To test this hypothesis, we studied the *Mdr2*-knockout mouse strain, which spontaneously develops cholestatic hepatitis followed by hepatocellular carcinoma[6], a prototype of inflammation-associated cancer[7]. We monitored hepatitis and cancer progression in *Mdr2*-knockout mice, and here we show that the inflammatory process triggers hepatocyte NF-κB through upregulation of tumour-necrosis factor-α (TNFα) in adjacent endothelial and inflammatory cells. Switching off NF-κB in mice from birth to seven months of age, using a hepatocyte-specific inducible IκB-super-repressor transgene, had no effect on the course of hepatitis, nor did it affect early phases of hepatocyte transformation. By contrast, suppressing NF-κB inhibition through anti-TNFα treatment or induction of IκB-super-repressor in later stages of tumour development resulted in apoptosis of transformed hepatocytes and failure to progress to hepatocellular carcinoma. Our studies thus indicate that NF-κB is essential for promoting inflammation-associated cancer, and is therefore a potential target for cancer prevention in chronic inflammatory diseases.

Hepatocellular carcinoma (HCC), the third leading cause of cancer mortality worldwide, commonly develops in the background of chronic hepatitis[8]. We confirmed and extended previous results[6,9], according to which tumour development in the *Mdr2*-knockout mouse, similarly to human HCC[8], progresses through distinct phases: inflammation, dysplasia, dysplastic nodules (adenoma-like), carcinoma and metastasis (Supplementary Fig. 1a, b). Hepatitis is the earliest sign of disease in the *Mdr2*-knockout mice, and is characterized by an extensive periductular and periportal mixed inflammatory infiltrate, rich in CD3-positive cells (Supplementary Fig. 1c).

NF-κB activation is often observed in human HCC, particularly following hepatitis[8]. The possibility that NF-κB activation is involved in *Mdr2*-knockout hepatocarcinogenesis was investigated by RelA (p65) immunostaining (Fig. 1a). Nuclear staining, indicative of NF-κB activation, was evident in knockout livers of mice at all ages, but not in normal, age-matched mice; this prompted a search for the source of NF-κB activation in the knockout mice. In some neoplasms such as Hodgkin's disease and certain lymphomas, NF-κB activation is an intrinsic, tumour autonomous feature, possibly related to mutations in its signalling pathway[10]. If a similar mechanism occurs in *Mdr2*-knockout HCC, one would observe nuclear NF-κB activation in all neoplastic hepatocytes. However, this was not the case; NF-κB activation appeared scattered at the parenchyma, predominantly adjacent to inflamed portal tracts (Fig. 1e, left panel), suggesting an inflammation-induced phenomenon. To evaluate this possibility, we fed knockout and wild-type mice with the non-steroidal anti-inflammatory drug (NSAID) ibuprofen for 10 days. This treatment resulted in decreased inflammation, evident by histological analysis (Fig. 1b), decreased serum alanine aminotransferase (ALT), a marker for hepatocyte damage, (Fig. 1c) and fewer neutrophils (Fig. 1c, d). p65 immunostaining showed that the degree of hepatocyte NF-κB activation in the NSAID-treated group was significantly lower than in the controls (Fig. 1e). In contrast, ibuprofen had no effect on hepatocyte NF-κB activation following intraperitoneal TNFα administration (data not shown). Hence, it seems that NF-κB activation in the knockout hepatocytes is secondary to parenchymal infiltration by inflammatory cells.

One likely mediator of NF-κB activation in the inflamed liver is TNFα, particularly its membrane form, which is upregulated in knockout livers (Fig. 2a). To study this possibility, we treated knockout mice with neutralizing anti-TNFα antibodies for three days and analysed hepatocyte NF-κB activation. Anti-TNFα treatment abolished hepatocyte p65 nuclear staining (Fig. 2b), confirming the prediction that NF-κB activation is primarily induced by TNFα. To determine the source of TNFα in the inflamed liver, we fractionated wild-type and knockout livers to hepatocytes (>80% purity by haematoxylin-and-eosin (H&E)) and other cells (<2% hepatocytes). Analysis of the two fractions for TNFα expression by real-time polymerase chain reaction (PCR) confirmed that the source of TNFα was the non-hepatocyte fraction, which expressed fivefold more TNFα than the corresponding fraction of wild-type mice (Fig. 2c).

To study the relationship between the TNFα-producing cells and NF-κB activation in the hepatocytes, liver sections were stained for both TNFα and p65 (Fig. 2d, f). TNFα expression was detected primarily at portal spaces, both in endothelial and inflammatory cells (Fig. 2d). Hepatocyte nuclear p65 staining was particularly abundant close to TNFα-positive portal spaces (Fig. 2f), indicating that hepatocyte NF-κB is activated through paracrine TNFα stimulation. To confirm the identity of the TNFα producers and distinguish them from TNFα-binding cells, liver sections of wild-type, knockout and ibuprofen-treated mice were analysed by *in situ* messenger RNA hybridization. Similar to the immunostaining data, TNFα mRNA was found to be highly expressed by endothelial and inflammatory cells of knockout mice, but far less in wild-type and ibuprofen-treated knockout mice. TNFα expression was hardly detected in either knockout or wild-type hepatocytes (Fig. 2e).

The frequent activation of NF-κB in knockout hepatocytes